Electronic Supporting Information

Exploring Catalyst Passivation with NMR Relaxation

Neil Robinson[‡], **Lynn F. Gladden and Carmine D'Agostino***

Department of Chemical Engineering and Biotechnology, University of Cambridge, Philippa Fawcett Drive, West Cambridge Site, Cambridge, CB3 0AS, UK

[‡] Presenting Author

* Corresponding Author. Email: cd419@cam.ac.uk

1. The Inversion Recovery Experiment

The inversion recovery pulse sequence is shown in Figure S1. The application of a 180° radio frequency (RF) pulse inverts the equilibrium magnetisation of the sample (which lies along the +z axis, parallel to the direction of the static magnetic field B_0) such that the spin magnetisation now lies along the –z axis. Spin-lattice relaxation causes longitudinal recovery of this magnetisation. After a given recovery time τ a 90° RF pulse rotates the recovering spin magnetisation into the transverse plane, inducing the measured NMR signal.

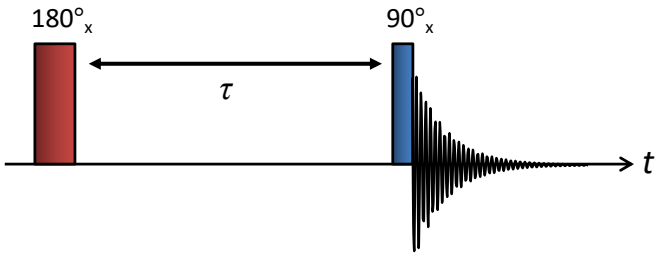

Figure S1. Inversion recovery pulse sequence.

The rate of recovery of longitudinal magnetisation is measured by altering the recovery delay period, typically through several orders of magnitude. In the present work we have used 16 logarithmically spaced τ delays. Fourier transformation of the resulting NMR signals leads to a number of NMR spectra differing only in signal intensity. Integration of the relevant spectral peaks across this range of spectra provides appropriate data from which a fit to Equation (6) in the main text may be acquired.

The following figures indicate the results of T_1 inversion recovery experiments performed across our range of samples.

1.1 Bulk Liquids

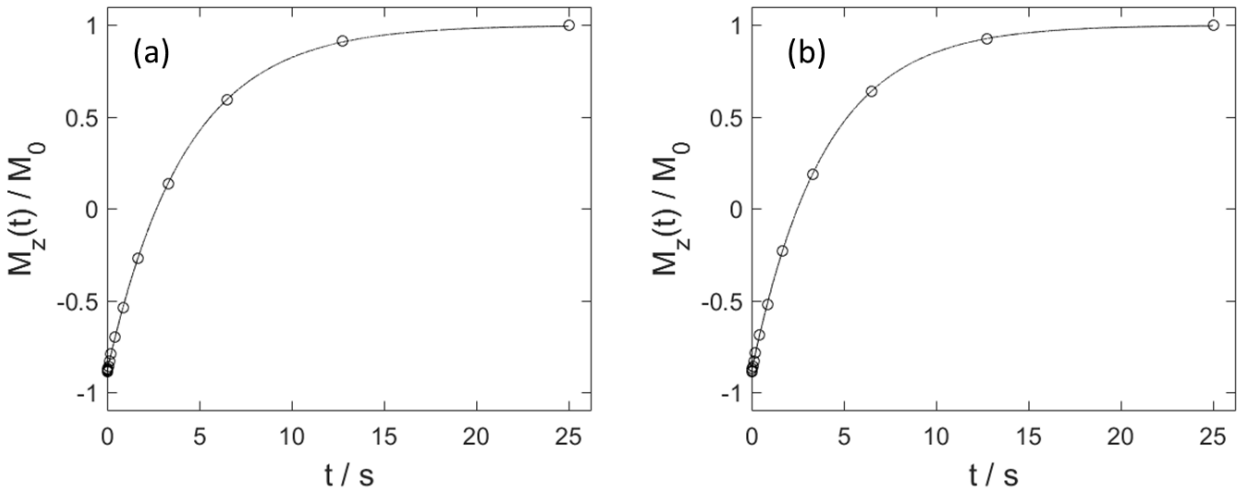

Figure S2. Inversion recovery curves for bulk methanol: a) methyl group with T_1 = 4.22 s and b) hydroxyl group with T_1 = 3.92 s.

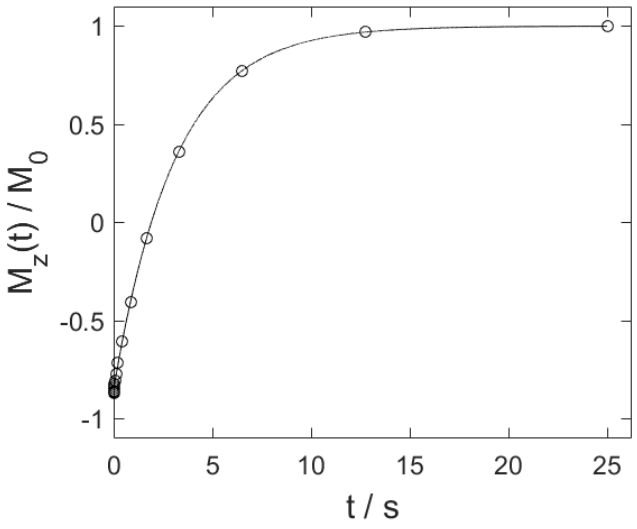

Figure S3. Inversion recovery curve for bulk cyclohexane with T_1 = 3.10 s.

1.2 Methanol-Saturated Oxides

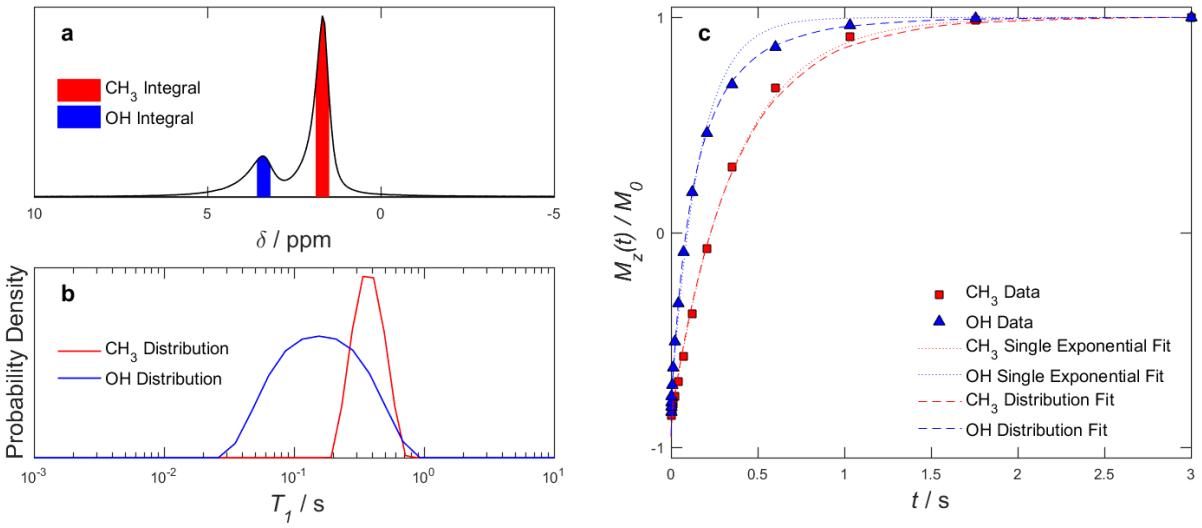

Figure S4. Methanol-saturated γ-Alumina: a) Methyl and hydroxyl peak integration limits b) Methyl and hydroxyl proton T_1 distributions c) Inversion recovery curves indicating the fits achieved through use of single T_1 values and the distributions shown in b).

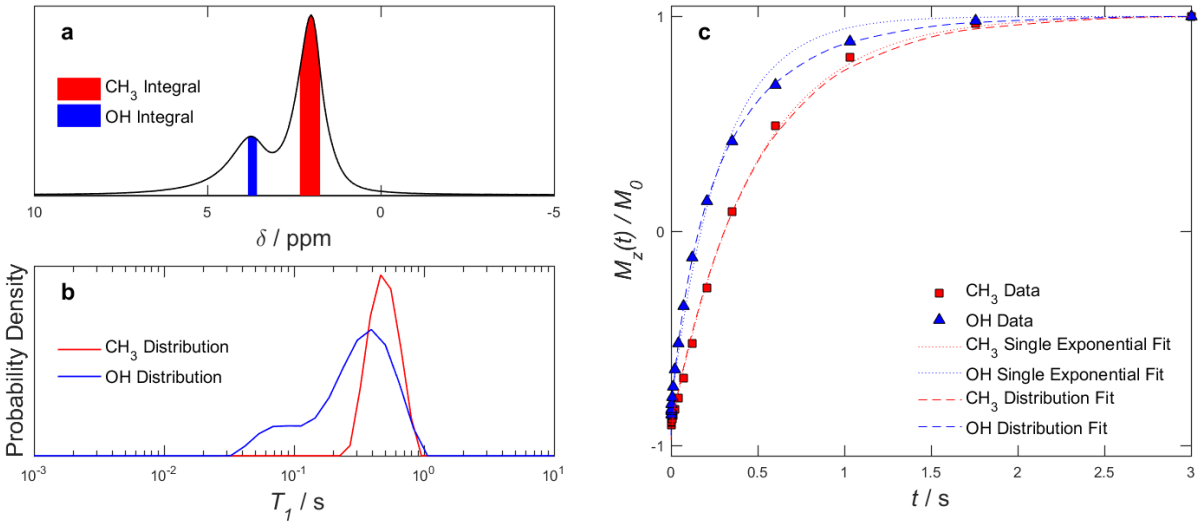

Figure S5. Methanol-saturated θ-Alumina: a) Methyl and hydroxyl peak integration limits b) Methyl and hydroxyl proton T_1 distributions c) Inversion recovery curves indicating the fits achieved through use of single T_1 values and the distributions shown in b).

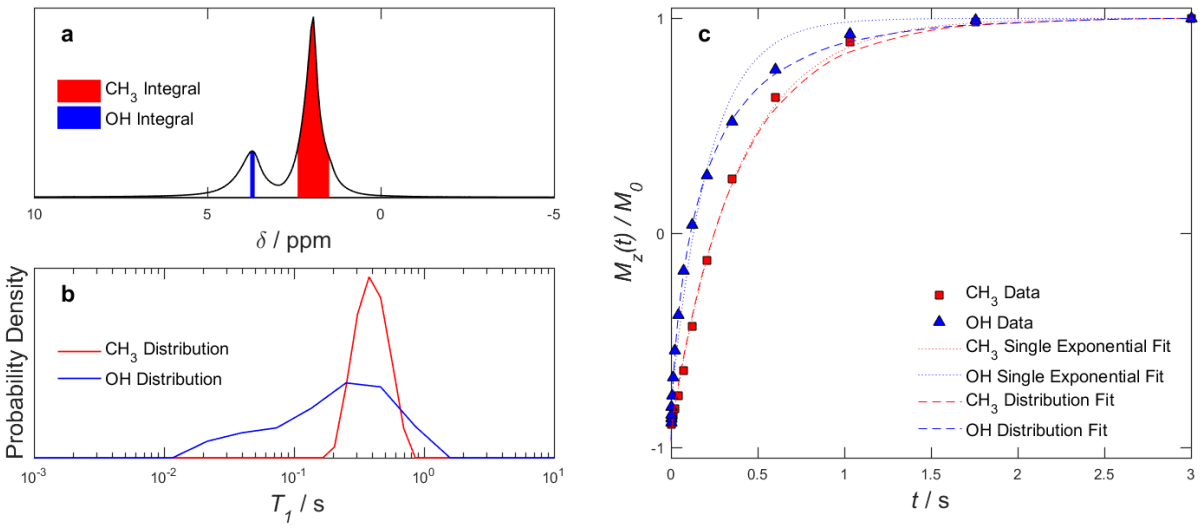

Figure S6. Methanol-saturated Anatase-Titania: a) Methyl and hydroxyl peak integration limits b) Methyl and hydroxyl proton T_1 distributions c) Inversion recovery curves indicating the fits achieved through use of single T_1 values and the distributions shown in b).

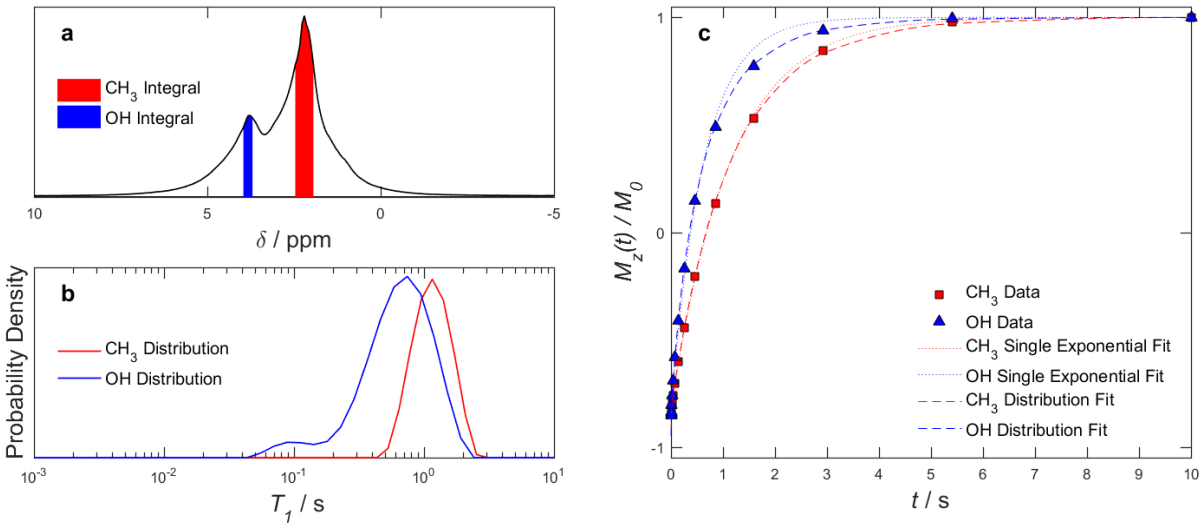

Figure S7. Methanol-saturated Silica: a) Methyl and hydroxyl peak integration limits b) Methyl and hydroxyl proton T_1 distributions c) Inversion recovery curves indicating the fits achieved through use of single T_1 values and the distributions shown in b).

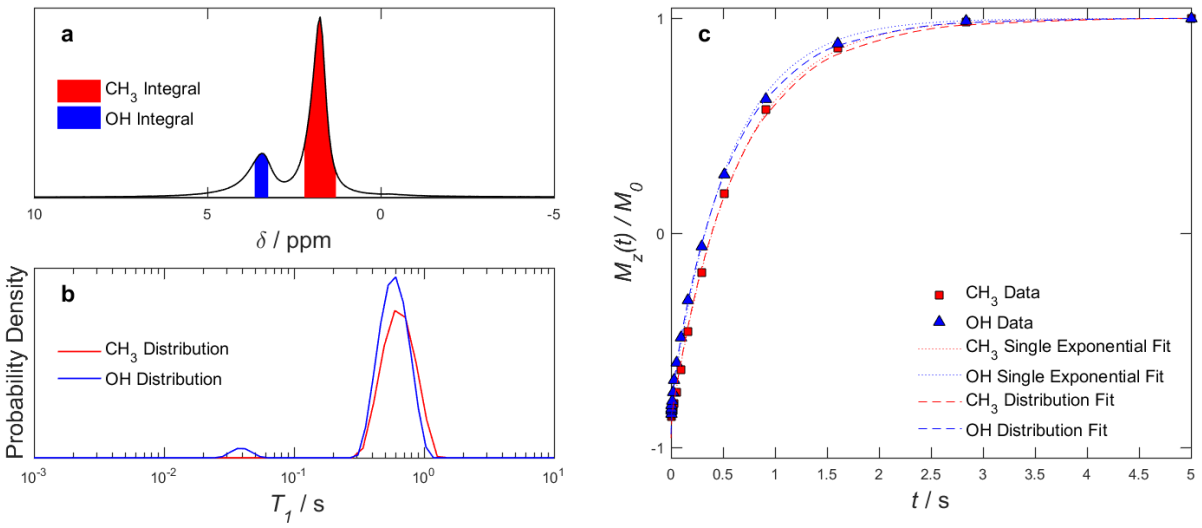

Figure S8. Methanol-saturated γ-Alumina-TEOS: a) Methyl and hydroxyl peak integration limits b) Methyl and hydroxyl proton T_1 distributions c) Inversion recovery curves indicating the fits achieved through use of single T_1 values and the distributions shown in b).

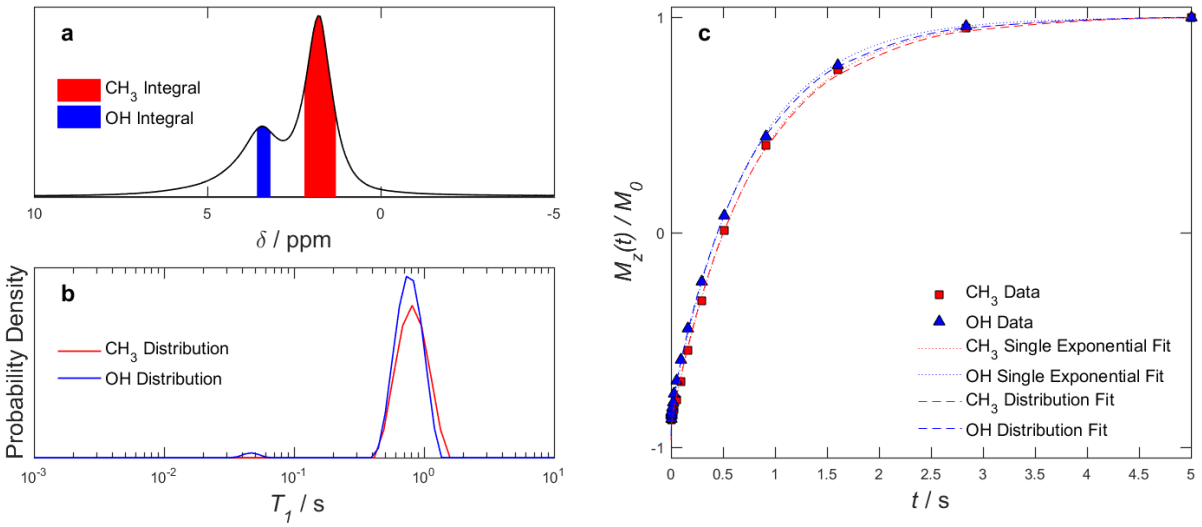

Figure S9. Methanol-saturated θ-Alumina-TEOS: a) Methyl and hydroxyl peak integration limits b) Methyl and hydroxyl proton T_1 distributions c) Inversion recovery curves indicating the fits achieved through use of single T_1 values and the distributions shown in b).

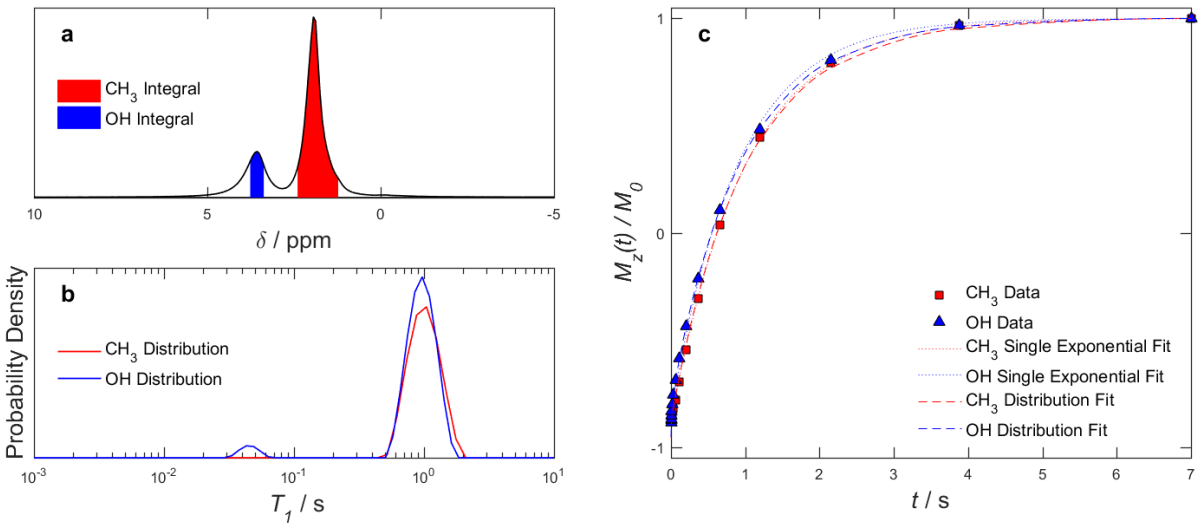

Figure S10. Methanol-saturated A-Titania-TEOS: a) Methyl and hydroxyl peak integration limits b) Methyl and hydroxyl proton T_1 distributions c) Inversion recovery curves indicating the fits achieved through use of single T_1 values and the distributions shown in b).

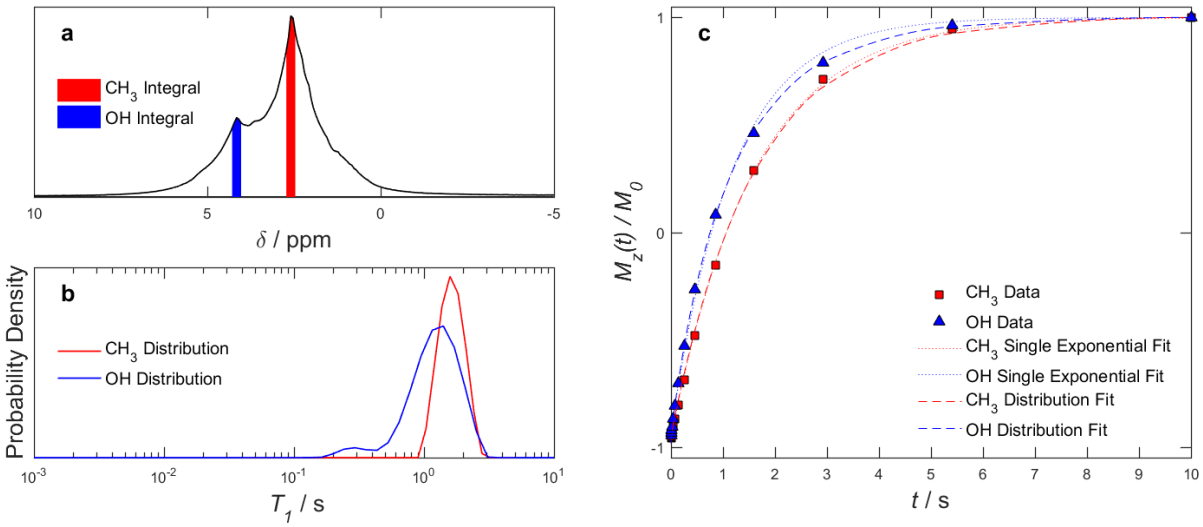

Figure S11. Methanol-saturated Silica-TEOS: a) Methyl and hydroxyl peak integration limits b) Methyl and hydroxyl proton T_1 distributions c) Inversion recovery curves indicating the fits achieved through use of single T_1 values and the distributions shown in b).

1.3 Cyclohexane-Saturated Oxides

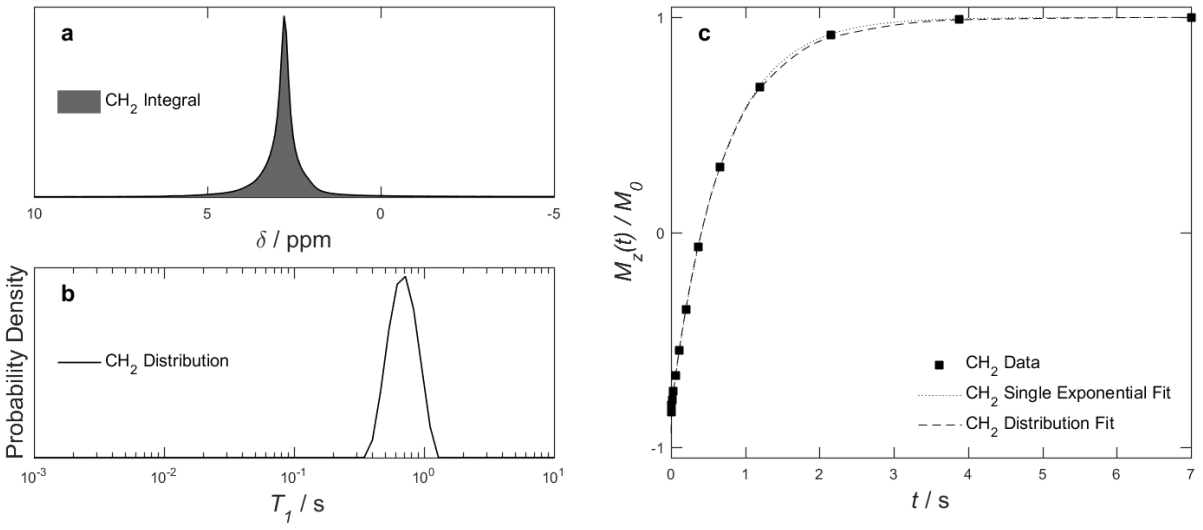

Figure S12. Cyclohexane-saturated γ-Alumina: a) Peak integration limits b) T_1 distribution c) Inversion recovery curves indicating the fits achieved through use of a single T_1 value and the distribution shown in b).

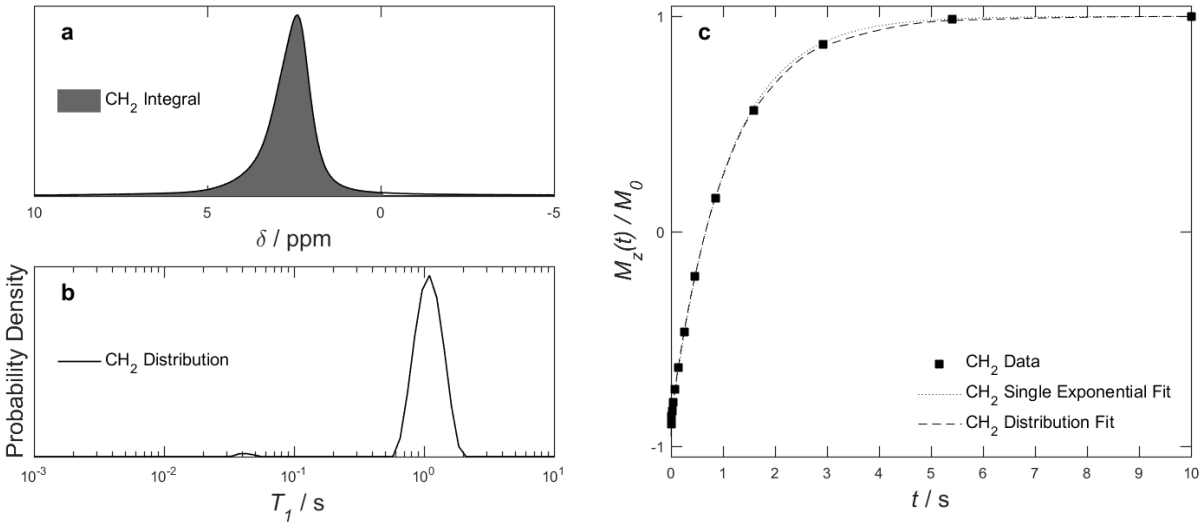

Figure S13. Cyclohexane-saturated θ-Alumina: a) Peak integration limits b) T_1 distribution c) Inversion recovery curves indicating the fits achieved through use of a single T_1 value and the distribution shown in b).

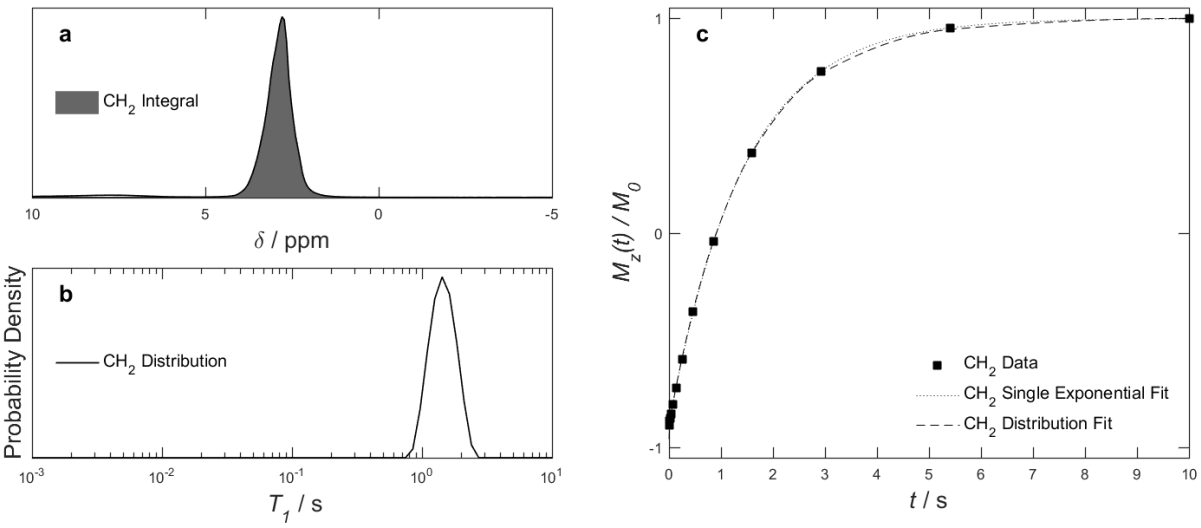

Figure S14. Cyclohexane-saturated A-Titania: a) Peak integration limits b) T_1 distribution c) Inversion recovery curves indicating the fits achieved through use of a single T_1 value and the distribution shown in b).

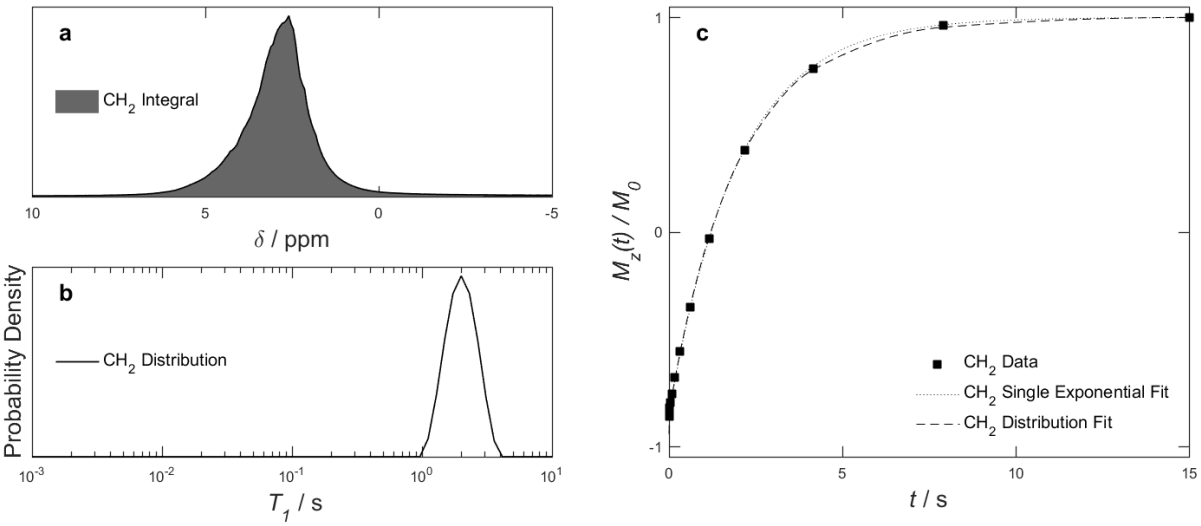

Figure S15. Cyclohexane-saturated Silica: a) Peak integration limits b) T_1 distribution c) Inversion recovery curves indicating the fits achieved through use of a single T_1 value and the distribution shown in b).

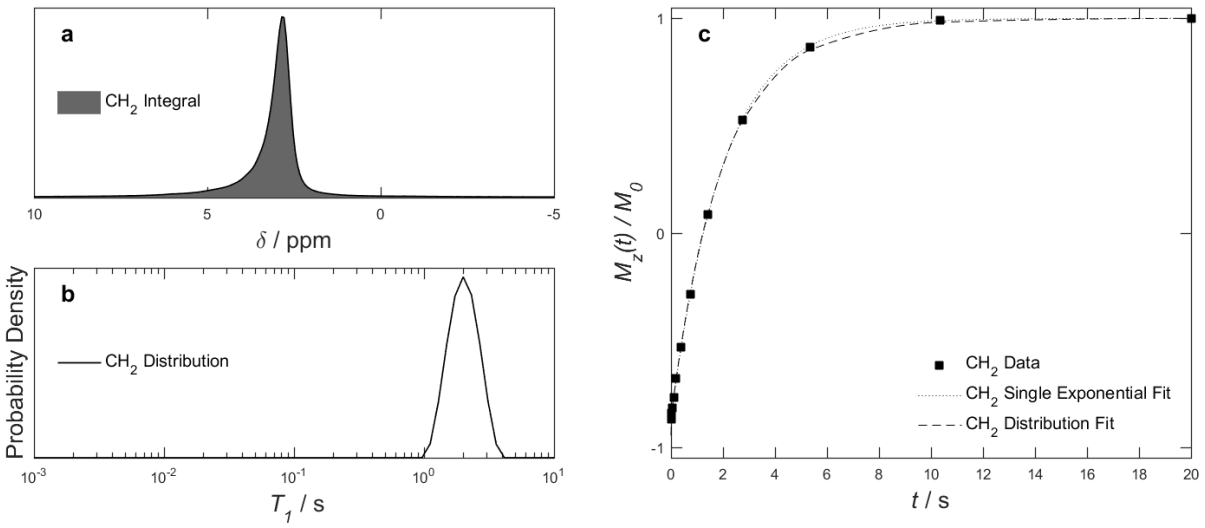

Figure S16. Cyclohexane-saturated γ-Alumina-TEOS: a) Peak integration limits b) T_1 distribution c) Inversion recovery curves indicating the fits achieved through use of a single T_1 value and the distribution shown in b).

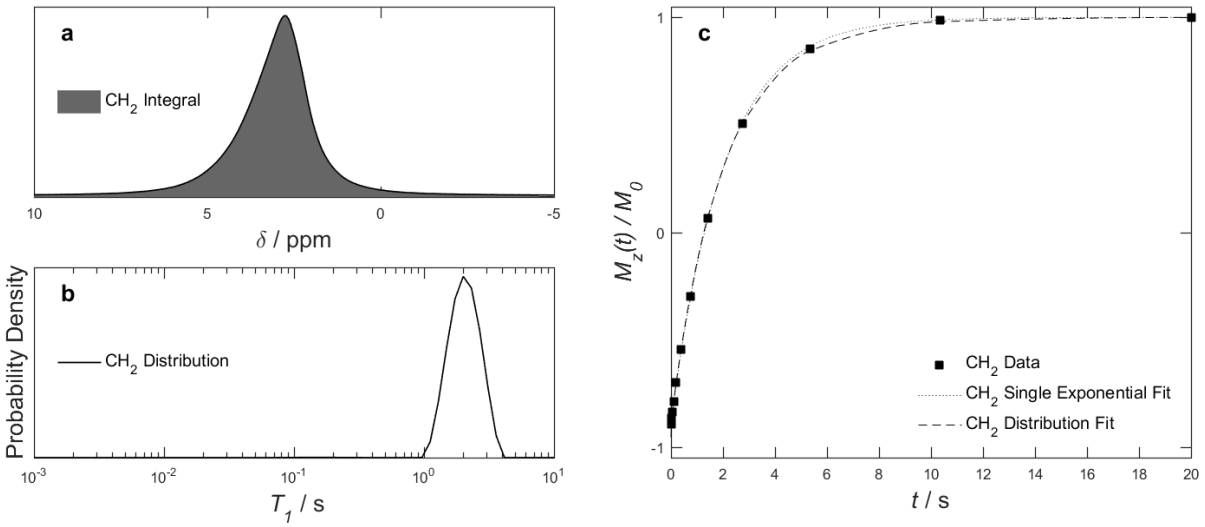

Figure S17. Cyclohexane-saturated θ-Alumina-TEOS: a) Peak integration limits b) T_1 distribution c) Inversion recovery curves indicating the fits achieved through use of a single T_1 value and the distribution shown in b).

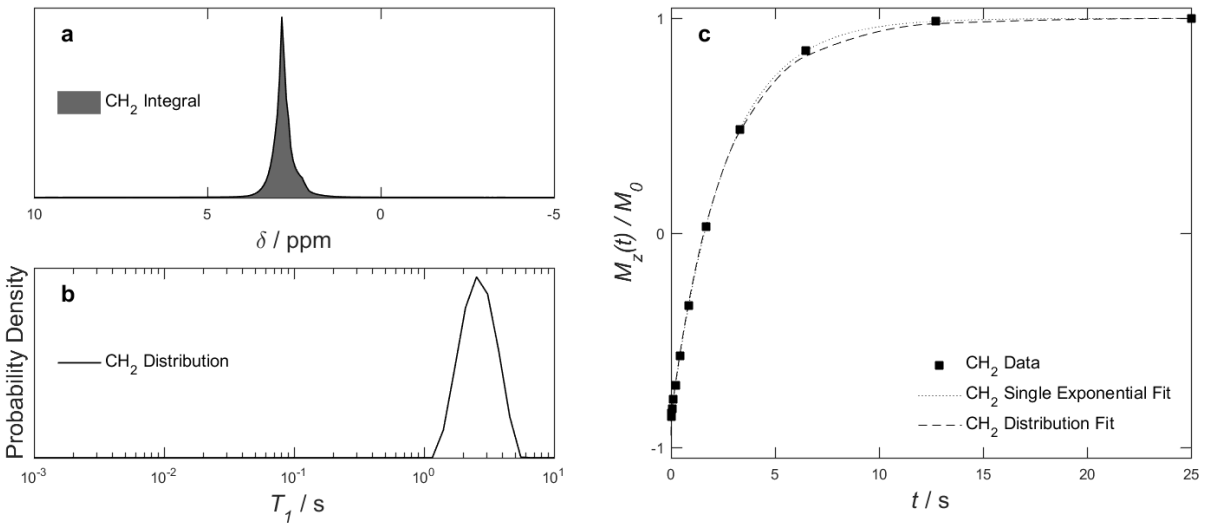

Figure S18. Cyclohexane-saturated A-Titania-TEOS: a) Peak integration limits b) T_1 distribution c) Inversion recovery curves indicating the fits achieved through use of a single T_1 value and the distribution shown in b).

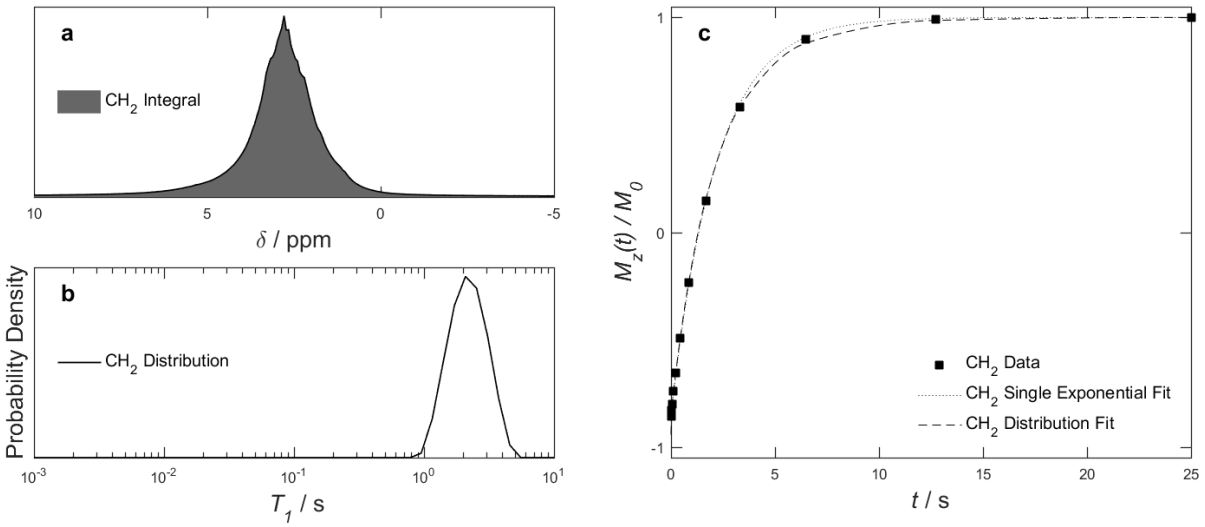

Figure S19. Cyclohexane-saturated Silica-TEOS: a) Peak integration limits b) T_1 distribution c) Inversion recovery curves indicating the fits achieved through use of a single T_1 value and the distribution shown in b).

2. Spin-Lattice Interaction Parameter

Figure S20 below displays the spin-lattice interaction parameter for cyclohexane-saturated (unpassivated) oxides.

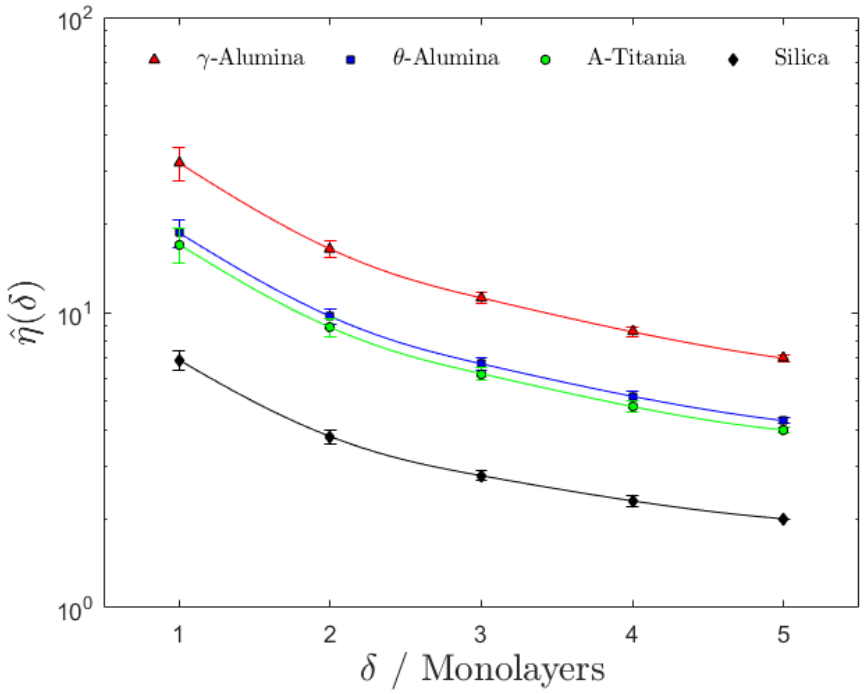

Figure S20. Rotational interaction parameter acquired for cyclohexane-saturated mesoporous oxides.